Active transport of oil droplets along oriented microtubules by kinesin molecular motors

Céline Bottier,*[a] Jacques Fattaccioli,[a] Mehmet C. Tarhan,[b] Ryuji Yokokawa,[cd] Fabrice O. Morin,[b] Beomjoon Kim,[b] Dominique Collard[a] and Hiroyuki Fujita[b]

Received 15th December 2008, Accepted 20th February 2009
First published as an Advance Article on the web 17th March 2009
DOI: 10.1039/b822519b

We demonstrate the active transport of liquid cargos in the form of oil-in-water emulsion droplets loaded on kinesin motor proteins moving along oriented microtubules. We analyze the motility properties of the kinesin motors (velocity and run length) and find that the liquid cargo in the form of oil droplets does not alter the motor function of the kinesin molecules. This work provides a novel method for handling only a few molecules/particles encapsulated inside the oil droplets and represents a key finding for the integration of kinesin-based active transport into nanoscale lab-on-a-chip devices. We also investigate the effect of the diameter of the droplets on the motility properties of the kinesin motors. The velocity is approximately constant irrespective of the diameter of the droplets whereas we highlight a strong increase of the run length when the diameter of the droplets increases. We correlate these results with the number of kinesin motors involved in the transport process and find an excellent agreement between our experimental result and a theoretical model.

Introduction

One of the fundamental problems for the continued miniaturization of lab-on-a-chip systems towards the next generation of nanodevices involves the efficient transport and assembly of materials in nanoscale systems. The scaling laws governing fluid flow and diffusion-based transport indicate that biomolecular motors are an effective option for actively transporting molecules or particles in nanodevices.[1–3]

Kinesin proteins, one type of biomolecular motor, are highly efficient nanoscale engines which play a critical role in a wide variety of biological processes including cell motility, cell division and intracellular transport.[4] They convert chemical energy derived from the hydrolysis of ATP into mechanical work allowing them to walk along microtubules. These filamentous polymers are cylindrical tubes measuring 24 nm in diameter[5] and up to tens of micrometres in length.

An exciting area of research aims at integrating motor protein-driven transport for controlled cargo manipulation on chips to sort or separate[6] an extremely small sample volume of analyte and/or assemble materials.[7–10] These *in vitro* developments are essential for miniaturizing high-throughput methods and bio-detection systems and for improving the understanding of molecular assembly processes through a bottom-up approach.

With the goal of creating lab-on-a-chip systems that exploit molecular motors for active transport, recent developments have succeeded in controlling the motor function *in vitro* such as the moving direction of the kinesin molecules. Since the progressive movement of the kinesin motors is directed towards the plus end (+) and away from the minus (−) end of the microtubules, the orientation of the filaments by polarity is necessary. Several methods allow for the active steering of microtubules such as pressure-driven flows,[11] viscous drag combined with gliding assay,[12] external electric[13] or magnetic[14] fields. Once the microtubules are oriented, the kinesin molecules are loaded with different types of cargo that can be moved in a controlled direction; this configuration corresponds to the natural geometry and is called the bead assay.[15]

Various types of solid particles have already been transported *in vitro* by kinesin molecules in a bead assay arrangement including microscopic beads,[16,17] quantum dots[18] and nanowires.[19] With a long-term view of harnessing motor proteins for sensitive screening, it is necessary to prevent target molecules from interacting with each other or with the environment during the transport process. This constraint demands the development of novel types of cargo such as containers in which target molecules or particles can be placed, and suggests working with liquid carriers.

In recent years colloidal emulsion droplets have been identified as good candidates for drug delivery systems.[20,21] Robust and extremely versatile,[22] they can be designed to hold volumes as small as a fraction of a femtolitre and therefore can encapsulate materials as diverse as hydrophilic[23] and hydrophobic[24] molecules or nanoparticles[25] in extremely small quantities. We propose here to actively transport oil-in-water emulsion droplets using kinesin molecules walking along oriented microtubules.

In this article, we describe the synthesis of functionalized micrometer-sized emulsion droplets and the method of transporting by kinesin motors. We demonstrate that the kinesin molecules can transport the oil droplets and examine the effect of the diameter of the droplets on both velocity and run length of the kinesin motors. Whereas the velocity is not affected, we find that increasing the diameter of the droplet leads to a strong

[a]*LIMMS/CNRS-IIS, Institute of Industrial Science, Tokyo University, 153-5805, Japan. E-mail: celine@iis.u-tokyo.ac.jp*
[b]*CIRMM, Institute of Industrial Science, Tokyo University, 153-5805, Japan*
[c]*Department of Micro System Technology, Ritsumeikan University, 525-8577, Japan*
[d]*PRESTO, JST, 332-0012, Japan*

increase of the run length. These results are discussed in relation with the number of kinesin motors, which are simultaneously attached to the microtubule and are therefore cooperatively involved in the active transport of the cargo.

Experimental

Purification of the proteins

The purification procedures of kinesin and tubulin have been described elsewhere.[12] Briefly we use two types of kinesin. The first type is a full-length histidine-tagged kinesin for the orientation of microtubules in the microchannel diluted at 0.13 mg mL^{-1} in 1/3 AC buffer: casein diluted at 0.7 mg mL^{-1} in BRB80 buffer (80 mM PIPES, NaOH (pH 6.8), 1 mM $MgCl_2$, 1 mM EGTA). The second type is a biotinylated kinesin we use to coat the functionalized emulsion droplets (diluted at 0.065 mg mL^{-1} in BRB80 buffer). We purify tubulin from porcine brains and store it in liquid nitrogen at a concentration of 4 mg mL^{-1}. We obtain microtubules by polymerizing tubulin at 37 °C for 30 min in a solution containing $MgSO_4$ (1 mM, Sigma) and GTP (Guanosine 5′-triphosphate, 1 mM, Sigma). We finally stabilize the resulting microtubules by paclitaxel (Taxol, 20 mM, Sigma) to prevent depolymerization.

Preparation of the emulsion

We obtain oil droplets by preparing a soybean oil-in-water emulsion stabilized by casein sodium salt from bovine milk.[26] At first we slowly incorporate the soybean oil (Sigma) in a casein sodium salt solution (13 wt % in purified deionized water, Sigma) until a mass fraction of oil $\Phi = 70\%$ is reached, resulting in a crude emulsion. Then we dilute the sample in purified deionized water until a mass fraction of oil $\Phi = 20\%$, rendering the emulsion less viscous and thus easier to handle.

At this stage, the emulsion is highly polydispersed with droplet diameters ranging between 5 and 20 μm. We decrease the size of the droplets with an ultrasonic probe (30 cycles of 5 s ON + 15 s OFF, power 3, Digital Sonifier, Branson, Danbury, USA). Finally we wash the emulsion four times to eliminate the unbound casein. Washing consists of diluting one volume of emulsion in one volume of carbonate/bicarbonate buffer (pH 8.3), centrifuging the mixture for 2 minutes in a table-top centrifuge (2000 g, Hitachi Koki Corp., Japan) and removing one volume of the lower phase to keep the initial droplet fraction.

Functionalization of the oil droplets

We are able to realize the functionalization of the oil droplets by streptavidin with a two-step approach. We first incubate 200 μL of the washed emulsion with 16 μL of biotin-X-NHS solution (0.02 mg mL^{-1} in DMSO, Calbiochem) for 30 min at room temperature. Biotin X-NHS binds to the amino groups of casein proteins through the formation of covalent peptide bonds. At the end of the reaction, we wash the emulsion three times with carbonate/bicarbonate buffer to remove unbound biotins. For the second step, we add 20 μL of streptavidin solution (Sigma, diluted at 0.1 mg mL^{-1} in PBS buffer: 150 mM NaCl, 10 mM Na_2HPO_4, 20 mM NaH_2PO_4, pH 7.4) and incubate the mixture for 10 min. Streptavidin binds to biotin-X-NHS due to a highly specific chemical affinity.[27] We present a schematic view of a functionalized droplet in Fig. 1A.

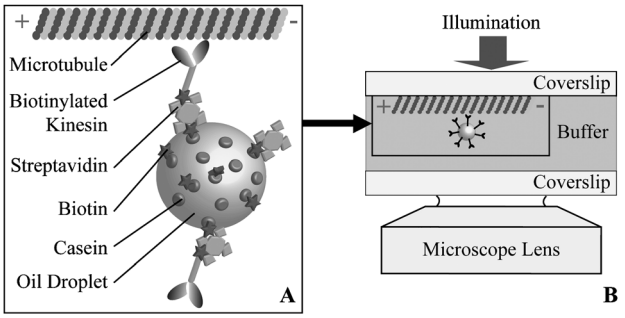

Fig. 1 (A) Schematic view of a kinesin-coated oil droplet. Biotin-X-NHS binds on the casein coating of the oil droplet through peptide bonds, then streptavidin attaches specifically on biotin-X-NHS. Finally biotinylated kinesin binds to the streptavidin coating of the oil droplet. The transport process is achieved in a bead assay configuration where the kinesin molecules walk along the microtubules from minus (−) to plus (+) ends. (B) Observation by DIC microscopy of the transport process of kinesin-coated oil droplets along oriented microtubules on the upper slide of a flow cell.

We determine the size distribution of the streptavidin-coated droplets by dynamic light scattering (DLS) measurements (ALV, Langen, Germany). Fitting the size distribution of the emulsion with a Gaussian curve yields a mean radius of 1 μm (data not shown).

Preparation of the flow cell with oriented microtubules

The kinesin molecules move from the minus (−) end to the plus (+) end of the microtubules. For this reason, it is necessary to orient the filaments by polarity to control the direction of the motion. We achieve the alignment of the microtubules using a polydimethylsiloxane (PDMS) microchannel as previously described.[12] Briefly we mould a PDMS microchannel on a SU-8 50 (Microchem.) structure patterned on a silicon wafer (height: 100 μm, width: 300 μm, length: 25 mm). Then we place the moulded PDMS slab on a glass slide coated with histidine-tagged kinesin and orient the microtubules by combining the gliding assay with a syringe pump-induced viscous drag.[12] After the orientation process, we immobilize the microtubules by first flowing 0.1% glutaraldehyde (incubation of 5 min, Sigma) and then 0.1 M glycine (incubation of 10 min, Wako) solutions to crosslink the contact points between the kinesins and the microtubules, and we remove the PDMS slab.

We perform the motility experiments in a flow cell consisting of two glass coverslips separated by grease-coated papers. As the oil droplets tend to float in the chamber (due to the difference in densities of water and oil), we prepare the flow cell by placing the slide containing the oriented microtubules on top of another slide (Fig. 1B). We transfer the slide containing the oriented microtubules manually while keeping it in aqueous environment. Observation of the glass slide containing fluorescent-labelled microtubules before and after the transfer shows that this process does not disturb the orientation of the filaments even if it causes a loss of microtubules (data not shown).

Motility assay of kinesin-coated oil droplets

For the kinesin motility assay, we dilute the functionalized emulsion by a factor of 10 in BRB80 buffer to avoid a high concentration of droplets in the flow cell. Then we prepare the kinesin-coated oil droplets by incubating 1 μL of biotinylated kinesin (0.065 mg mL^{-1}) with 5 μL of diluted streptavidin-coated oil droplets for 15 min. The kinesin motors cover the surface of the oil droplets through the specific avidin–biotin interaction.[27]

After the preparation of the flow cell with the oriented microtubules on the upper slide, we inject the kinesin-coated oil droplets in the chamber and leave them undisturbed for 10 min allowing them to bind onto the microtubules. We wash out unbound oil droplets by flowing BRB80 buffer. As a last step, we add ATP solution (adenosine 5′-triphosphate, 1 mM, Sigma) into the flow cell to activate the transport process.

Estimation of the number of kinesins per droplet

Considering the mean radius of the droplets ($R = 1$ μm, $V_{droplet} = 4.2 \times 10^{-12}$ cm^3), the density of the oil ($\rho_{soybean\ oil} = 0.92$ g cm^{-3}, $M_{droplet} = 3.85 \times 10^{-12}$ g) and the oil fraction in the emulsion solution (56.10^{-3} g of oil in 200 μL of emulsion solution), we estimate the number of oil droplets in a certain volume of emulsion sample.

We use a large excess of sodium caseinate to stabilize the emulsion leading to a maximal casein surface coverage of 3 mg m^{-2}.[28] We consider the number of available amino groups per casein molecule[29] and the molecular weight of casein[30] to be 12 and 23 000 g mol^{-1}, respectively. Considering the surface area of one droplet, we approximate the number of amino groups available to bind to biotin molecules. For the functionalization of the droplets, we add biotin-X-NHS and then streptavidin to the emulsion sample. We assume that all biotin molecules bind to the amino groups of casein[31] and all streptavidin molecules bind to the biotin molecules.[32] Under these conditions, streptavidin is the limiting reagent leading to a coating of 1.5×10^3 streptavidin molecules per droplet.

For the last step, we add kinesin molecules (120 000 g mol^{-1}) in excess compared with the number of available streptavidin molecules. Assuming that all streptavidins are bound with biotinylated kinesins, the kinesin degree of coating is equal to the streptavidin one: 1.5×10^3 kinesins per droplet. Again considering the surface area of the droplet, the coverage is 120 kinesins μm^{-2} corresponding to a mean area of 90×90 nm^2 per single kinesin motor. In a close contact configuration, the estimated area occupied by a single kinesin is ~ 300 nm^2.[33]

Image acquisition and data analysis

We used an inverted microscope (Olympus IX-71) with a 100x oil immersion objective (Uplan Apo, Olympus) for the observations. We perform the motility assays at room temperature (22–25 °C) and monitor the experiments using a differential interference contrast (DIC) setup on a microscope stage with a photometrics camera (Cascade 512 II), controlled by Metamorph imaging software (Universal Imaging Corp.). We acquire images with an exposure time of 30 ms in time-lapse mode (2 frames every 1 s). We manually measure the velocity, the run length and the diameter of the oil droplets (±0.1 μm) using Adobe ImageReady software.

Results and discussion

Visualization of the transport process

To determine the transport properties of the kinesin-driven oil droplets, we perform bead assays using an array of oriented and immobilized microtubules. The kinesin-driven droplets

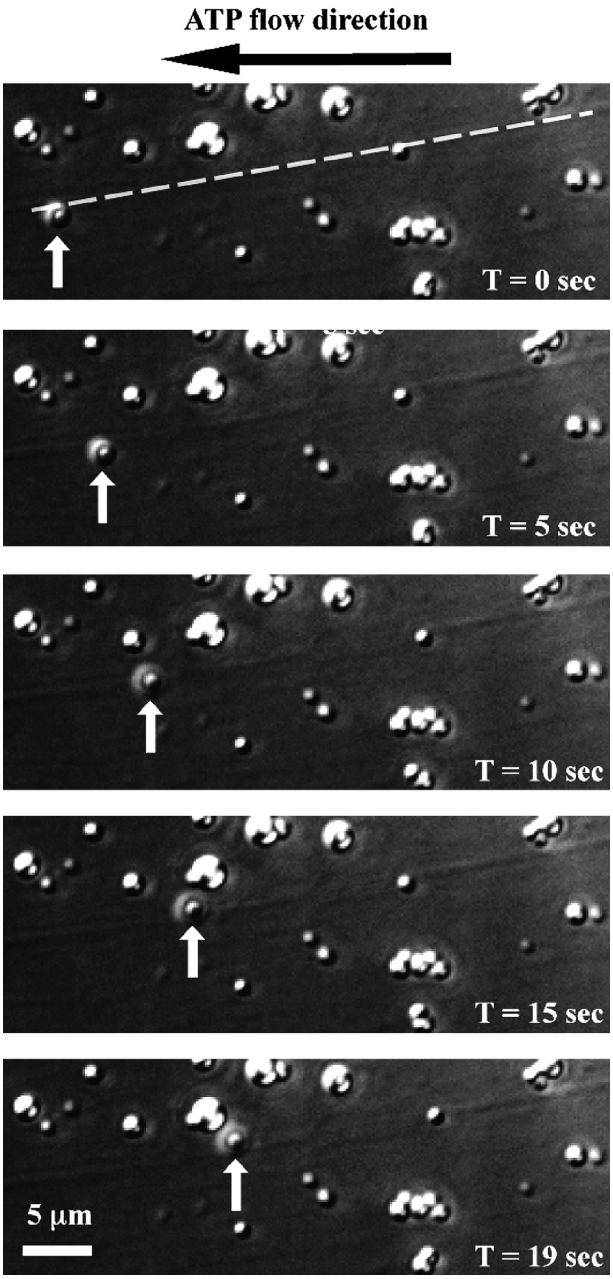

Fig. 2 Successive photographs of the same area taken in DIC microscopy showing the successful transport of a kinesin-coated oil droplet along a microtubule after the addition of 1 mM ATP. The white arrows track the position of the droplet whereas the ATP flow direction is indicated with the black arrow. A white dotted line is added on the first photograph to indicate the location of the microtubule. Scale bars: 5 μm.

experience linear and one-dimensional movements. We present an example of a successful transport process in Fig. 2 where successively taken photographs show the motion of a kinesin-driven oil droplet along a microtubule. The cargo moves continuously in the opposite direction of the ATP flow proving that the motion is due to the kinesin motility and not due to liquid flow. This droplet covers a distance of 13.5 μm in 19 s resulting in a velocity of 710 nm s^{-1}.

In total, we observe 70 successful events in nine different flow cells. For the area we present in Fig. 2, the number of successful events is rather low: after addition of ATP, only one droplet out of more than 20 droplets experiences motion. Two plausible explanations that can account for this observation are the low density of microtubules and the adhesive interactions between the droplets and the substrate.[34] Due to the density difference between oil and water, we transfer the glass slide containing the oriented microtubules to use it as the upper slide of the flow cell (see experimental section) causing a loss of microtubules (data not shown). The probability for kinesin-coated droplets of binding to a microtubule is therefore reduced. Moreover, as soon as the droplets arrive in the vicinity of the substrate they strongly adhere to it preventing diffusion into the flow cell and the eventual binding to a microtubule.

The micrometre-sized and liquid oil droplets do not disturb the function of the kinesin motors

To analyze the oil droplet transport process, we first examine the motor velocity of 70 successful events. We calculate the velocity of cargo that we observe to be moving continuously during time scales ranging from 2 to 60 s. Fitting a single Gaussian peak to the histogram of the velocities of the 70 events yields an average velocity of 450 ± 30 nm s^{-1} (mean ± standard error (SE)), as shown in Fig. 3A.

Different types of solid particles have already been carried in a bead assay configuration. The mean velocities reported in the literature are: 740[16] and 220 to 280 nm s^{-1},[17] 280 nm s^{-1},[18] and 600 nm s^{-1},[19] for beads, quantum dots and nanowires, respectively. The method for measuring the velocity differs between all of these studies explaining the dispersion of the reported values. For example, in our work, velocity is determined for continuous motion only, whereas in other cases[17] data are collected by averaging velocities for several seconds, regardless of periods of cargo immobility and thus resulting in a slower velocity.

The second metric we analyze is the run length, or the distance motors travel along microtubules before detaching or stopping. We report the run lengths of 66 events on a histogram and fit the data to a single exponential curve, as shown in Fig. 3B.[35] Of the 70 events, 4 trials with run lengths of 1 μm are not included in the distribution to better fit the data and avoid an overestimation of the mean run length. The average run length corresponds to the decay constant of the exponential fitting function, which in our case is 4.8 μm. This value is comparable to the mean run length of 4.5 μm reported for microspheres.[17]

The mean velocity and run length of the oil droplets are in the same range as the values reported for solid particles. We therefore conclude that attaching liquid cargos to the biotinylated kinesins does not disturb the motor function by interfering with the kinesin–microtubule interaction. Despite the micrometre-sized liquid and oil droplets, the kinesin activity is not affected.

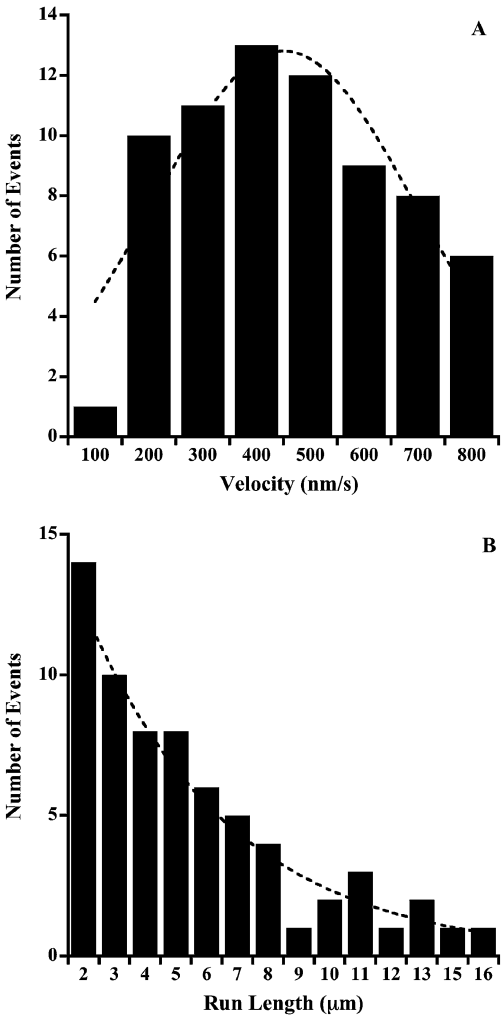

Fig. 3 Velocity and run length distributions of the kinesin-coated oil droplets measured over nine flow cells. (A) Histogram of the velocities (N = 70). The dotted line is a Gaussian fit of the distribution with its center position at 450 ± 30 nm s^{-1} (mean ± SE). (B) Histogram of the run lengths > 1 μm (N = 66). The dotted line is the exponential fit of the distribution giving a mean run length of 4.8 μm.

Effect of the diameter of the oil droplet on both velocity and run length

Among the 70 successful transportation events, the diameters of the droplets vary from 0.5 to 2.0 μm. We do not detect any motion when the diameter of the droplet exceeds 2 μm but this does not mean that the transportation is not possible above this value. As the electrostatic interactions increase with the diameter of the droplets, the adhesion of large droplets to the substrate may be enhanced, thus significantly decreasing the probability of observing the motion of large droplets.[36]

To analyze the effect of the diameter of the droplets on both velocity and run length, we sort the oil droplets according to their diameters into four groups: 0.5, 1.0, 1.5 and 2.0 μm. In each group, we calculate the average diameter and the mean velocity or mean

run length and add the standard errors on the X and Y-axis. We present the variations of the velocity and run length as a function of the diameter of the droplets in Fig. 4A and 4B, respectively.

We report the velocities of all observed events ($N = 70$, Fig. 4A) whereas we only take into account the run lengths of 25 of those events (Fig. 4B). Indeed, we often observe adhesive interactions between the droplets and the substrate leading to the immobilization of the cargo. In these cases, it is not possible to determine if the walking mechanism stops because of the inactivity of the motors or because of adhesive interactions between the cargo and the substrate. Therefore, we only present the events showing a droplet transported which subsequently detaches from the microtubule.

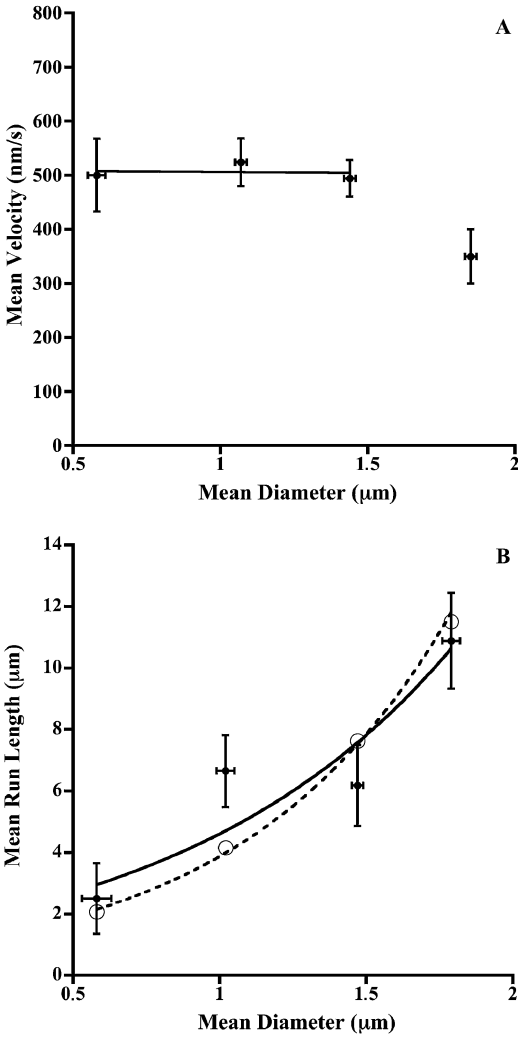

Fig. 4 Variations of the mean velocity (A) and mean run length (B) of the kinesin-coated oil droplets as a function of the droplet diameter ± SE. The solid lines are the linear fits to mean velocities ± SE ($N = 70$) and mean run lengths ± SE ($N = 25$) up to 1.5 μm, respectively. (B) We plot the theoretical curve (dotted line) corresponding to the model proposed by Klumpp and Lipowsky.[37] These authors express the theoretical run length (μm) as: $(5^{N-1})/N$, where N is the number of pulling motors. According to the values of the average diameters ($d = 0.58$, 1.02, 1.47 and 1.79 μm), we calculate the active lines (nm) (see Fig. 5). As explained in the text, we estimate that a single kinesin motor occupies an area of 90 × 90 nm^2. By simply dividing the values of the active lines by 90, we obtain the number of motors involved in the transport process: $N = 1.83$ for $d =$ 0.58 μm, $N = 2.44$ for $d = 1.02$ μm, $N = 2.93$ for $d = 1.47$ μm and $N =$ 3.25 motors for $d = 1.79$ μm. The four open circles correspond to the theoretical run lengths, which are calculated using the number of motors N cited above.

Fitting the velocities by a linear relation for diameters up to 1.5 μm indicates that the speed of the kinesin motors is not affected by the size of the oil droplets (Fig. 4A). The mean velocity found by the linear fit is 500 nm s^{-1}. However, for the droplets of 2.0 μm diameter, the mean velocity is reduced to 350 nm s^{-1}. We exclude the effect of viscous drag, as this force is negligible in this range of velocity. At the present time, we do not provide any satisfactory explanation and believe that further experiments are required to fully explain this phenomenon.

Whereas the size of the droplets does not influence the mean velocity of the kinesin motors, we observe a significant increase of the mean run length when increasing the diameter of the droplets (Fig. 4B). The mean run length varies from 2.5 μm to 10.8 μm for droplet diameters of 0.5 μm and 2.0 μm, respectively. In other words the larger the cargo, the farther it travels. We believe that this counterintuitive observation is strongly related to the number of droplet-bound motors, which are simultaneously attached to the microtubule and therefore cooperatively involved in the active transport of the cargo.

To elucidate this question, we estimate the number of pulling motors according to the size of the droplet. We assume that the density of kinesin motors is constant irrespective of the diameter of the droplet. This consideration implies that the larger the droplet, the more motors are involved in the active transport. As described by Beeg *et al.*, the kinesin molecules are able to extend between the microtubule and the cargo.[16] By geometric consideration, these authors assess that motors may bind to the microtubule if their distances from it do not exceed 16 nm. Applying a similar geometric consideration to our case, we calculate the "active line" that we define as the one-dimensional curvature of the droplet where the kinesin molecules may bind to the microtubule and thus be simultaneously active in the transport process (Fig. 5A).

The difference in the curvature of small and big droplets implies that the active line of large droplets is longer than for small droplets. We approximate the active lines to be 150 nm (dotted line) and 310 nm (solid line) for droplet diameters of 0.5 and 2.0 μm, respectively (Fig. 5B). As explained in the experimental part, we estimate that a single kinesin motor occupies an area of 90 × 90 nm^2 on the surface of the droplet. By simply dividing the value of the active lines by 90, we can estimate the number of the motors involved in the transport process: ~1.7 and ~ 3.4 motors for droplets of 0.5 and 2.0 μm diameter, respectively.

In a theoretical study, Klumpp and Lipowsky express the mean run length in micrometres (RL) as a function of the number of pulling motors (N) as: $\mathrm{RL} = 5^{N-1}/N$.[37] We present on Fig. 4B (dotted line) the theoretical curve corresponding to this model and we highlight an excellent agreement between our experimental data and that proposed by Klumpp and Lipowsky.[37]

Moreover, our results corroborate a recent theoretical and experimental study showing that the travelling distance of 100 nm diameter beads is strongly increased when more motors are involved in the transport process.[16] Thus, the kinesin motors

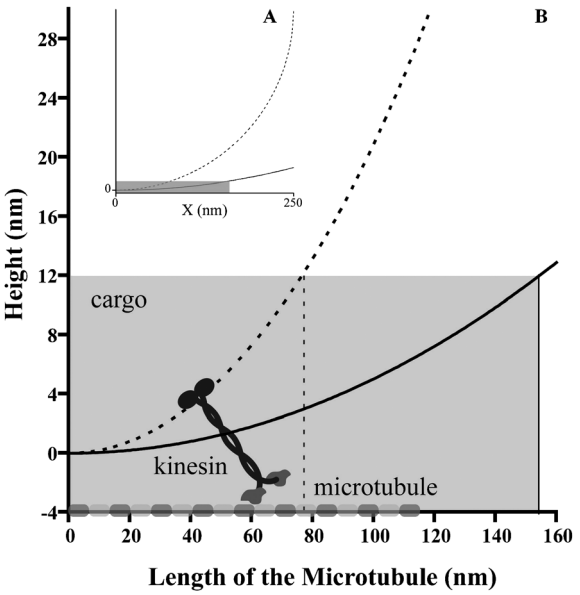

Fig. 5 Schematic model showing the determination of the "active lines" defined as the one-dimensional curvatures of the droplets where the kinesin molecules are involved in the transport process. (A) Curvatures of two droplets of 0.5 μm (dotted line) and 2.0 μm (solid line) diameters. We enlarge the grey area in (B). (B) We consider that motors can bind to the microtubule if their distances from it do not exceed 16 nm.[16] We approximate the active lines to their projections on the X-axis: 150 nm (2 × 75) and 310 nm (2 × 155) for oil droplet diameters of 0.5 μm (dotted line) and 2.0 μm (solid line), respectively. For clarity, we add schematic representations of the kinesin and the microtubule that are not drawn to scale.

show a similar physical behaviour when they are loaded with nanometre-sized and solid beads[16] or micrometre-sized and liquid droplets. We conclude that the critical parameter determining the motility properties of the kinesins is the number of pulling motors and not the nature of the loaded cargo.

Conclusion

We demonstrate that micrometre-sized droplets can be transported in a bead assay arrangement using kinesin motors that walk along microtubules. The values of the mean velocity and run length of the kinesin-driven oil droplets are in the same range as other types of solid particles. The diameter of the droplets does not affect the velocity whereas it has a significant impact on the run length, which strongly rises when the size of the droplet increases. We explain this phenomenon by consideration of the number of kinesin motors, which are simultaneously involved in the transport process and we highlight an excellent agreement between our experimental results and a theoretical model proposed by Klumpp and Lipowsky.[37]

From a biophysical point of view, a recent study shows the production of emulsion droplets where both size and composition of ligands are controlled.[34] Applying this strategy to our emulsion droplets would enable us to propose a particularly suitable system to precisely study the impact of the size of the cargo and the number of pulling motors on the motion properties of kinesin. Moreover, the micrometer-sized droplets offer a large surface area that can be saturated with kinesin motors and may lead to a strong increase in the run length, which is of great importance for the integration of molecular motors into synthetic devices. This strategy also opens new opportunities for transporting cargo over long distances showing that the bead assay configuration can compete with the gliding assay arrangement.[38] Moreover, compared with the gliding assay where the molecules are attached to the microtubules, our system allows control of the amount of target molecules, which could be potentially transported in the droplet. Indeed, when the carrier is the microtubule itself, it is not possible to control the number of molecules attached on the filament, as its length is constantly changing due to polymerizing and depolymerizing processes.

From an engineering point of view, these results strongly support our overall and long-term goal to exploit the active transport of emulsion droplets to handle a very small number of target molecules and to dynamically assemble nanocomposite materials encapsulated in droplets. Combining the kinesin-based active motion of emulsion droplets with interconnected networks of oriented microtubules for a two-dimensional transport system[39] may lead to an extremely controlled nanoscale assembly system.

Acknowledgements

We thank The Japan Society for the Promotion of Science (JSPS, fellowships #PE07503 and #P08724 for C. Bottier and #P06733 for J. Fattaccioli) and The Ministry of Education, Culture, Sports, Science and Technology, Japan (scholarship for M. C. Tarhan). We also gratefully acknowledge Pr. H. Tanaka and M. Leocmach, Institute of Industrial Science, The University of Tokyo, for Dynamic Light Scattering measurements and M. Cordero, Institute of Industrial Science, The University of Tokyo, for corrections of this manuscript.

References

1 H. Hess and V. Vogel, *Rev. Mol. Biotechnol.*, 2001, **82**, 67–85.
2 T. Nitta and H. Hess, *Nano Lett.*, 2005, **5**, 1337–1342.
3 M. G. L. van den Heuvel and C. Dekker, *Science*, 2007, **317**, 333–336.
4 R. D. Vale, *Cell*, 2003, **112**, 467–480.
5 E. Nogales, M. Whittaker, R. A. Milligan and K. H. Downing, *Cell*, 1999, **96**, 79–88.
6 C. T. Lin, M. T. Kao, K. Kurabayashi and E. Meyhofer, *Nano Lett.*, 2008, **8**, 1041–1046.
7 H. Hess, G. D. Bachand and V. Vogel, *Chem. Eur. J.*, 2004, **10**, 2110–2116.
8 J. Clemmens, H. Hess, R. Doot, C. M. Matzke, G. D. Bachand and V. Vogel, *Lab Chip*, 2004, **4**, 83–86.
9 H. Hess, J. Clemmens, C. Brunner, R. Doot, S. Luna, K. H. Ernst and V. Vogel, *Nano Lett.*, 2005, **5**, 629–633.
10 H. Hess, *Soft Matter*, 2006, **2**, 669–677.
11 T. B. Brown and W. O. Hancock, *Nano Lett.*, 2002, **2**, 1131–1135.
12 R. Yokokawa, S. Takeuchi, T. Kon, M. Nishiura, K. Sutoh and H. Fujita, *Nano Lett.*, 2004, **4**, 2265–2270.
13 M. G. L. van den Heuvel, M. P. de Graaff and C. Dekker, *Science*, 2006, **312**, 910–914.
14 B. M. Hutchins, M. Platt, W. O. Hancock and M. E. Williams, *Small*, 2007, **3**, 126–131.
15 S. M. Block, L. S. B. Goldstein and B. J. Schnapp, *Nature*, 1990, **348**, 348–352.
16 J. Beeg, S. Klumpp, R. Dimova, R. S. Gracià, E. Unger and R. Lipowsky, *Biophys. J.*, 2008, **94**, 532–541.
17 R. Yokokawa, M. C. Tarhan, T. Kon and H. Fujita, *Biotechnol. Bioeng.*, 2008, **101**, 1–8.

18 G. Muthukrishnan, B. M. Hutchins, M. E. Williams and W. O. Hancock, *Small*, 2006, **2**, 626–630.
19 L. Jia, S. G. Moorjani, T. N. Jackson and W. O. Hancock, *Biomed. Microdevices*, 2004, **6**, 67–74.
20 G. M. Lanza, K. D. Wallace, M. J. Scott, W. P. Cacheris, D. R. Abendschein, D. H. Christy, A. M. Sharkey, J. G. Miller, P. J. Gaffney and S. A. Wickline, *Circulation*, 1996, **94**, 3334–3340.
21 P. M. Winter, S. D. Caruthers, A. Kassner, T. D. Harris, L. K. Chinen, J. S. Allen, E. K. Lacy, H. Zhang, J. D. Robertson, S. A. Wickline and G. M. Lanza, *Cancer Res.*, 2003, **63**, 5838–5843.
22 J. Bibette, F. Leal-Calderon, V. Schmitt and P. Poulin, in *Emulsion Science: Basic Principles, an overview*. Ed. Springer Verlag, 2002.
23 J. A. Hanson, C. B. Chang, S. M. Graves, Z. Li, T. G. Mason and T. J. Deming, *Nature*, 2008, **455**, 85–88.
24 M. A. Neves, H. S. Ribeiro, I. Kobayashi and M. Nakajima, *Food Biophysics*, 2008, **3**, 126–131.
25 S. K. Mandal, N. Lequeux, B. Rotenberg, M. Tramier, J. Fattaccioli, J. Bibette and B. Dubertret, *Langmuir*, 2005, **21**, 4175–4179.
26 L. Bressy, P. Hébraud, V. Schmitt and J. Bibette, *Langmuir*, 2003, **19**, 598–604.
27 N. M. Green, *Biochem. J.*, 1963, **89**, 599–609.
28 Y. Fang and D. G. Dalgleish, *J. Colloid Interface Sci.*, 1993, **156**, 329–334.
29 X. Pan, M. Mu, B. Hu, P. Yao and M. Jiang, *Biopolymers*, 2006, **81**, 29–38.
30 G. A. Morris, I. M. Sims, A. J. Robertson and R. H. Furneaux, *Food Hydrocolloids*, 2004, **18**, 1007–1014.
31 I. M. Grumbach and R. W. Veh, *J. Immunol. Methods*, 1991, **140**, 205–210.
32 N. M. Green, *Methods Enzymol.*, 1990, **184**, 51–67.
33 L. A. Amos, *J. Cell Sci.*, 1987, **87**, 105–111.
34 J. Fattaccioli, J. Baudry, N. Henry, F. Brochard-Wyart and J. Bibette, *Soft Matter*, 2008, **4**, 2434–2440.
35 R. D. Vale, T. Funatsu, D. W. Pierce, L. Romberg, Y. Harada and T. Yanagida, *Nature*, 1996, **380**, 451–453.
36 J. N. Israelachvili, in *Intermolecular and surface forces*, Second Edition, Academic Press, London, 1992.
37 S. Klumpp and R. Lipowsky, *Proc. Natl. Acad. Sci. USA*, 2005, **102**, 17284–17289.
38 J. Clemmens, H. Hess, J. Howard and V. Vogel, *Langmuir*, 2003, **19**, 1738–1744.
39 R. K. Doot, H. Hess and V. Vogel, *Soft Matter*, 2007, **3**, 349–356.

